Coherent laser detection by frequency-shifted optical feedback

E. Lacot, R. Day, and F. Stoeckel
Laboratoire de Spectrométrie Physique, Université Joseph Fourier de Grenoble, CNRS, Boîte Postale 87, 38402 Saint Martin d'Hères Cedex, France

(Received 16 February 2001; published 19 September 2001)

The dynamical response of a laser to frequency-shifted optical feedback is investigated both theoretically and experimentally. The ultrahigh sensitivity of a class-*B* laser (i.e., a laser with a cavity damping rate γ_c higher than the population damping rate γ_1) to external light injection is demonstrated by the optical detection of weak optical feedback. Compared to a conventional optical beating, the intensity modulation induced by the coherent interaction between the laser electric field and the frequency-shifted reinjected electric field can be several orders of magnitude higher. This method permits high sensitive interferometry and hence imaging. We call this laser detection technique laser optical feedback imaging (LOFI). When the optical frequency shift is resonant with the laser relaxation frequency, the intracavity amplification of the beating is maximum and the enhancement is given by the laser damping rate ratio γ_c/γ_1. This amplification is of the order of 10^6 for a microchip laser. We also show that without optical feedback the strong fluctuations of the laser output power are well described by the Langevin noise process. In a broad range around the laser relaxation frequency the laser quantum noise is also resonantly amplified and is then several orders of magnitude higher than the detector noise. In these conditions, the LOFI is a shot noise limited detection technique. Reflectivity as low as 10^{-13} is then easily detectable with a laser output power of a few milliwatts with a detection bandwidth of 1 kHz. Experimentally, for weak optical feedback the laser fluctuations are principally composed of the LOFI modulation signal at the shifted frequency and of the laser quantum noise amplified at the relaxation frequency. For strong optical feedback, nonlinear effects appear in the laser dynamics. In these conditions, harmonics and parametrics peaks appear in the power spectrum. The LOFI detection system is then saturated.

DOI: 10.1103/PhysRevA.64.043815 PACS number(s): 42.60.Mi, 42.62.−b, 42.79.Qx

I. INTRODUCTION

Laser properties and behavior can be significantly affected and modified by optical feedback [1,2]. The electrical field reinjected into the laser cavity is highly coherent when the beam is reflected by a mirror but can be partially or weakly coherent if it is reinjected from a diffusing surface or volume. Since the discovery of the laser, parasitic coherent optical feedback has been the source of serious laser problems, increasing noise and creating laser instabilities [3]. On the other hand, controlled optical feedback can be of practical use. For example, linewidth narrowing and improved frequency stability can be obtained [3].

Potential applications are also possible. One of these is laser feedback interferometry (LFI), where the steady-state intensity of a laser is modified by coherent optical feedback from an external surface [4]. This induced change is dependent on the reflectivity, distance, and motion of the target. The first LFI device for distance and velocity measurement was demonstrated in 1963 by King and Steward [5,6]. In subsequent years, this phase-sensitive technique has been used to determine the direction of the target motion [7], to measure the laser axial mode number [8], for velocimetry [9], for laser frequency stabilization [10], and in metrology [11,12].

It is not always possible to have a mirror as a reflector in such applications. Noncooperative targets, such as diffusing surfaces or volumes or absorbing surfaces, have to be used on some occasions [13]. In these cases, the reinjected light is only partially spatially and/or temporally coherent. The nature of such light reduces drastically the interference effects occurring inside the laser cavity. The challenge is then to increase the observable signal in order to overcome this problem.

One solution is then to use the laser dynamics which are more sensitive to optical feedback than changes in the laser steady state. In 1964 Kleinman [14] suggested that a weak external signal applied to a class-*B* laser (solid-state laser or semiconductor laser) which exhibits relaxation oscillations during the onset of laser oscillation, can drastically influence the temporal laser spiking pattern. For example, high-dimensional chaos and controllable chaos can easily be provoked [15,16]. More recently Otsuka [2] reported the analysis of a laser response to Doppler-shifted optical feedback. The sensitivity of such a laser to optical feedback is proportional to the ratio γ_c/γ_1, where γ_c and γ_1 are, respectively, the damping rate of the laser cavity and of the population inversion. For typical solid-state or semiconductor lasers, values of this ratio are of the order of 10^3 while for a microchip laser, the value is as high as 10^6 which makes such lasers very interesting for experiments based on weak optical feedback [17–19]. This high sensitivity has been used in a self-mixing laser Doppler velocimetry (LDV) experiment [20]. The maximum of the modulation was obtained when the Doppler-shifted frequency was resonant with the laser relaxation oscillation frequency. In this condition, an optical feedback level as low as −170 dB (compared to the intracavity power) has been detected [21].

In this work we use the properties of a class-*B* laser to enhance the optical interference signal for analyzing and imaging noncooperative target properties. Hereafter, we call this detection technique LOFI, which stands for laser optical

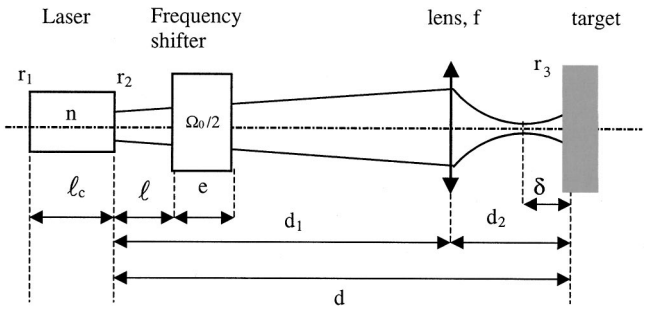

FIG. 1. Principle of the laser detection with frequency-shifted optical feedback.

feedback imaging. We describe and study a simple system that needs no expensive equipment and no complex optical alignment and which allows measurements of reflectivity, distances, velocities, vibrations, etc. with a high degree of accuracy.

This paper is organized as follows. In the theoretical section, we determine the ultimate sensitivity of a class-*B* laser with coherently shifted optical feedback. First, we determine, the coupling coefficient between the reinjected feedback electric field and the intracavity electric field. Then we give the rate equations governing the dynamics of a laser in the presence of frequency-shifted optical feedback. The laser quantum noise is described by standard Langevin forces. By solving the rate equations with a linear approximation, we determine the amplitude and the phase of the output modulation induced by both the frequency-shifted optical feedback (i.e., the signal) and by the Langevin forces (i.e., the noise). The theoretical signal to noise ratio is given and its dependence on the frequency shift is discussed.

In the experimental section, we briefly describe the LOFI experiment. The frequency dependence of the LOFI signal to noise ratio is compared to the theoretical result and the ultimate sensitivity is determined.

II. THEORY

Let us consider the case of a reinjected beam with an optical frequency shift Ω_0. Figure 1 shows the principle of such a laser experiment with the optical feedback shifted in frequency by Ω_0. l_c is the length of the laser cavity, n is the gain medium refractive index, l is the distance between the laser and the frequency shifter, and e its thickness. $R_1=|r_1|^2$, $R_2=|r_2|^2$ are the power reflectivity of the laser cavity mirrors, $d=d_1+d_2$ is the distance between the output coupler R_2 and the target, δ is the distance between the image waist and the target, and f is the focal length of the lens. The target has an effective self-reflectivity of $R_3=|r_3|^2$

A. Auto-injected laser

1. Basic equations

In the case of weak optical feedback ($r_3 \ll 1$), the following equations describe the behavior of the laser [1]:

$$\frac{dN}{dt}=\gamma_1(N_0-N)-BN|E(t)|^2+F_N(t), \tag{1}$$

$$\frac{d}{dt}E(t)e^{i\omega t}=[i\omega_c+\tfrac{1}{2}(BN-\gamma_C)]E(t)e^{i\omega t} + \gamma_{\text{ext}}E(t-\tau)e^{i\omega(t-\tau)}+F_E(t),$$

where we have added an external feedback term to the complex form of the standard laser equation [22].

Here, N is the population inversion, $E(t)$ is the complex amplitude of the electric field in reduced units (photon units), ω_c is the laser cavity frequency which is presumed resonant with the atomic frequency ($\omega_c=\omega_a$), ω is the optical running laser frequency, B is the Einstein coefficient, $\gamma_1 N_0$ is the pumping rate, γ_1 is the decay rate of the population inversion, and γ_c is the laser cavity decay rate. The laser quantum fluctuations are described by the conventional Langevin noise terms F_N and F_E [23]. The optical feedback is characterized by two parameters: the first one, $\tau=2d/c$, is the photon round-trip time between the laser and the target and the second one, γ_{ext}, is the reinjection rate of the feedback electric field. As derived in the Appendix, the coefficient γ_{ext} is related to the cavity damping rate γ_c and to reflectivity of the target r_3 as

$$\gamma_{\text{ext}}=\gamma_c\sqrt{R_{\text{eff}}}, \tag{2}$$

where $R_{\text{eff}}=|gr_3|^2$ is the effective reflectivity of the target and g is the coupling coefficient taking into account the overlapping of the retrodiffused field with the Gaussian cavity beam. In the above expression of the coupling rate γ_{ext} the multiple reflections between the laser and the target have been neglected.

2. Steady state

The stationary lasing conditions can be obtained from the set of Eqs. (1) by neglecting the noise terms and by setting the complex electric field E and the population inversion N to be constant. Without optical feedback ($\gamma_{\text{ext}}=0$), the steady-state solutions are given by

$$N_S=\gamma_c/B, \quad I_S=|E_S|^2=E_{\text{sat}}^2(\eta-1), \quad \omega=\omega_c, \tag{3}$$

where I_s is the stationary intensity of the laser field, $I_{\text{sat}}=E_{\text{sat}}^2=\gamma_1/B$ is the saturation intensity, and $\eta=BN_0/\gamma_c$ is the normalized pumping rate. At this point, we notice that the mean optical phase Φ_s of the laser field does not appear in the steady-state solutions. This means that the phase is not determined or is randomly distributed over 2π. We can therefore arbitrarily fix the mean value of the phase to $\Phi_s=2\pi$, which is quite convenient since the steady-state electric field becomes real.

With optical feedback, $\gamma_{\text{ext}}\neq 0$, the steady-state solutions are given by

$$N_s'=\frac{\gamma_c-2\gamma_{\text{ext}}\cos(\omega'\tau)}{B}, \tag{4a}$$

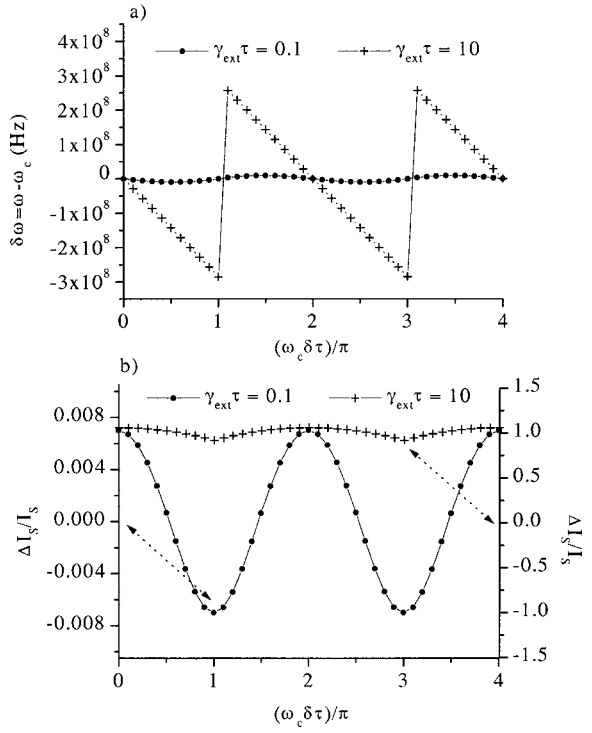

FIG. 2. Laser steady state versus change in time delay $\delta\tau$ for two values of the optical coupling parameter $\gamma_{ext}\tau=0.1$ ($R_{eff}=3\times10^{-6}$) and $\gamma_{ext}\tau\approx10$ ($R_{eff}=3\times10^{-2}$) and with $\omega_c=1.78\times10^{15}\,s^{-1}$, $\gamma_c=5.7\times10^9\,s^{-1}$, $\tau=1\times10^{-8}$ s ($d=1.5$ m). (a) Laser detuning frequency $\delta\omega=\omega'-\omega_c$, (b) relative change of the stationary intensity $\Delta I_s/I_s=I_s'-I_s/I_s$.

$$I_s'=|E_s'|^2=E_{sat}^2\frac{\eta-1+2(\gamma_{ext}/\gamma_c)\cos(\omega'\tau)}{1-2\dfrac{\gamma_{ext}}{\gamma_c}\cos(\omega'\tau)}, \tag{4b}$$

$$\omega'=\omega_c-\gamma_{ext}\sin(\omega'\tau). \tag{4c}$$

In the case of weak optical feedback ($\gamma_{ext}\tau\ll1$), Eq. (4c) shows that the laser optical frequency is not really affected by the external cavity ($\delta\omega=\omega'-\omega_c\cong0$) [Fig. 2(a)]. Equation (4b) becomes

$$I_s'=I_S\left(1+2\frac{\eta}{\eta-1}\frac{\gamma_{ext}}{\gamma_c}\cos(\omega_c\tau)\right). \tag{5}$$

The stationary intensity is therefore modulated by a weak interference effect [Fig. 2(b)]. In the case of strong optical coupling ($\gamma_{ext}\tau\gg1$), Eq. (4c) shows that the laser can be multimode. The laser optical frequency is now given by the longitudinal mode having the maximum gain of the compound cavity. For this mode, the oscillation condition is given by ($\cos\omega'\tau\cong1$). Figure 2(a) shows that the frequency detuning varies linearly with the length of the compound cavity. In this condition, Eq. (4b) becomes

$$I_S'=I_S\left(\frac{1+\dfrac{2}{\eta-1}\dfrac{\gamma_{ext}}{\gamma_c}}{1-2\dfrac{\gamma_{ext}}{\gamma_c}}\right). \tag{6}$$

The modulation of the stationary intensity is now crushed.

B. Frequency-shifted optical feedback

1. Basic equations

Let us consider now the case of a reinjected beam with an optical frequency shift Ω_0. We write the intracavity field as $E(t)e^{i\omega t}=E_c(t)e^{i\Phi_c(t)}e^{i\omega t}$, where $E_c(t)$ and $\Phi_c(t)$ are, respectively, the slowly varying amplitude and the optical phase. After a round-trip time τ, the reinjected electric field inside the laser cavity is given by $E_c(t-\tau)e^{i\Phi_c(t-\tau)}e^{i(\omega+\Omega_0)t}e^{-i[\omega+(\Omega_0/2)]\tau}$. In the interests of simplicity, we have supposed that the frequency shifter is as near as possible to the laser cavity ($l\ll d$) and has also a very small width ($e\ll d$). The set of Eqs. (1) can then be rewritten ignoring the Langevin's noise terms,

$$\frac{dN}{dt}=\gamma_1(N_0-N)-BN|E_c(t)|^2,$$

$$\frac{dE_c(t)}{dt}=\frac{1}{2}(BN-\gamma_c)E_c(t)+\gamma_{ext}\cos\left[\Omega_0 t-\left(\omega+\frac{\Omega_0}{2}\right)\tau-\Phi_c(t)+\Phi_c(t-\tau)\right]E_c(t-\tau), \tag{7}$$

$$\frac{d\Phi_c(t)}{dt}=\omega_c-\omega+\gamma_{ext}\sin\left[\Omega_0 t-\left(\omega+\frac{\Omega_0}{2}\right)\tau-\Phi_c(t)+\Phi_c(t-\tau)\right]\frac{E_c(t-\tau)}{E_c(t)}.$$

We now suppose that the effect of the feedback on the detuning of the cavity is weak [$\omega'\cong\omega_c$, see Eq. (4c)]. Hereafter we only consider the case where the round-trip time outside the cavity is shorter than the period of the frequency shift ($\Omega_0\tau\ll1$); this implies that $E_c(t-\tau)\cong E_c(t)$ and $\Phi_c(t-\tau)\cong\Phi_c(t)$. Equations (7) can be simplified to

$$\frac{dN}{dt}=\gamma_1(N_0-N)-BN|E_c|^2,$$

$$\frac{dE_c}{dt}=\frac{1}{2}[BN-\gamma_c+2\gamma_{ext}\cos(\Omega_0 t-\omega_c\tau)]E_c, \tag{8}$$

$$\frac{d\Phi_c}{dt}=\gamma_{ext}\sin(\Omega_0 t-\omega_c\tau).$$

The set of Eqs. (8) shows that both the net gain and the optical phase of the laser are modulated at the heterodyne frequency Ω_0. The amplitude of the modulation is propor-

tional to $\gamma_{\rm ext}$, which depends on the target properties while the phase shift $\omega_c\tau$ of the modulation depends on the target position.

2. LOFI signal

Solutions of Eqs. (8) for small variations can be obtained by linearization. If $\Delta_N(t)$, $\Delta_{E_c}(t)$, and $\Delta_{\Phi_c}(t)$ are small fluctuations around the stationary values, we can write

$$N(t)=N_S+\Delta_N(t),$$
$$E_C(t)=E_s+\Delta_{E_c}(t), \tag{9}$$
$$\Phi_c(t)=2\pi+\Delta_{\Phi_c}(t),$$

where N_s and E_s are given by Eqs. (3). By substituting Eqs. (9) into Eqs. (8) and neglecting second-order terms, we obtain the following set of linearized equations:

$$\frac{d\Delta_N}{dt}=-(\gamma_1+B|E_S|^2)\Delta_N-2BN_SE_S\Delta_{E_c},$$
$$\frac{d\Delta_{E_c}}{dt}=\frac{1}{2}BE_S\Delta_N+\gamma_{\rm ext}\cos(\Omega_0t-\omega_c\tau)E_s,$$
$$\frac{d\Delta_{\Phi_c}}{dt}=\gamma_{\rm ext}\sin(\Omega_0t-\omega_c\tau). \tag{10}$$

By solving Eqs. (10), we obtain $\Delta_{E_c}(t)$. The photon output rate (i.e., number of photons per second) is simply given by

$$n_{\rm out}(t)=\gamma_c|E_c(t)|^2. \tag{11}$$

The relative laser output power of the modulation is then given by

$$\frac{\Delta n_{\rm out}(t,\Omega_0)}{\langle n_{\rm out}(t)\rangle}=\frac{2\Delta_{E_c}(t,\Omega_0)}{E_s}$$
$$=2\gamma_{\rm ext}\frac{\sqrt{(\eta\gamma_1)^2+\Omega_0^2}}{\sqrt{(\omega_r^2-\Omega_0^2)^2+(\eta\gamma_1)^2\Omega_0^2}}$$
$$\times\cos(\Omega_0t-\omega_c\tau+\phi_r), \tag{12a}$$

where $\langle n_{\rm out}\rangle$ is the averaged photon output rate, $\omega_r=\sqrt{\gamma_1\gamma_c(\eta-1)}$ is the relaxation frequency of the laser, and ϕ_r is an additional phase shift which is independent of the nature ($\gamma_{\rm ext}$) and the position (τ) of the target and is defined by

$$\tan\phi_r=\frac{\Omega_0[(\omega_r^2-\Omega_0^2)-(\eta\gamma_1)^2]}{\eta\gamma_1\omega_r^2}.$$

We see from this signal that the effective reflectivity $R_{\rm eff}$ and the position d of the target can be determined, respectively, from the LOFI amplitude term and the LOFI phase $\omega_c\tau$.

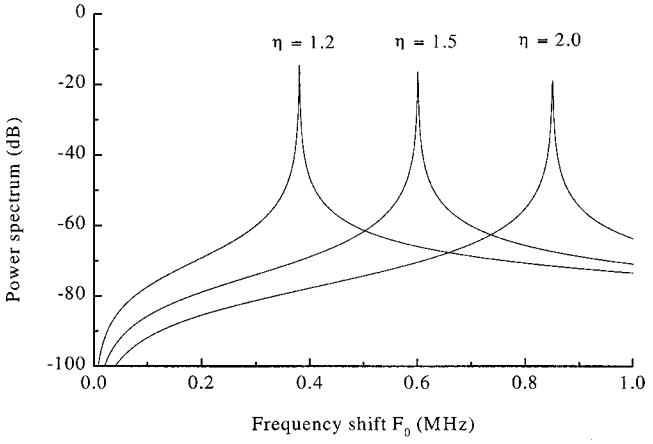

FIG. 3. Power spectrum in dB of the square of the relative amplitude of the modulation $\Delta n_{\rm out}/n_{\rm out}$ versus the frequency shift ($F_0=\Omega_0/2\pi$) for different values of the pump parameter η, with $\gamma_1=5\times10^3\ {\rm s}^{-1}$, $\gamma_c=5.7\times10^9\ {\rm s}^{-1}$, $R_{\rm eff}=10^{-14}$.

Moreover, the optical phase of the lasing electric field is

$$\Delta_{\Phi_c}(t,\Omega_0)=-\frac{\gamma_{\rm ext}}{\Omega_0}\cos(\Omega_0t-\omega_c\tau). \tag{12b}$$

Figure 3 shows the theoretical power spectrum of the square of the relative amplitude of the modulation $\Delta n_{\rm out}/n_{\rm out}$. As we can see, the power spectrum exhibits a strong resonance at the laser relaxation frequency ω_r with a full width at half maximum (FWHM) given by $\Delta_{\Omega_{1/2}}=\eta\gamma_1$. At the resonance frequency, the maximum relative amplitude of modulation is

$$\frac{\Delta n_{\rm out}(\omega_r)}{\langle n_{\rm out}\rangle}\cong\frac{2\gamma_{\rm ext}}{\eta\gamma_1}=2\frac{\gamma_c}{\eta\gamma_1}\sqrt{R_{\rm eff}}. \tag{13}$$

Compared to a standard heterodyne detection, an amplification of $\gamma_c/\eta\gamma_1$ occurs. For a microchip laser [25], γ_c/γ_1 is typically of the order of 10^6. Assuming a pumping rate of $\eta=2$, a relative amplitude of a 100% modulation is obtained for a feedback corresponding to a reflectivity as low as $R_{\rm eff}=10^{-12}$. The high sensitivity of the LOFI detection technique comes from this resonant amplification. For a zero-frequency shift, Eq. (12a) becomes

$$\frac{\Delta n_{\rm out}(t,\Omega_0=0)}{\langle n_{\rm out}(t)\rangle}=2\frac{\eta}{\eta-1}\frac{\gamma_{\rm ext}}{\gamma_c}\cos(\omega_c\tau), \tag{14}$$

which is identical to Eq. (5) obtained previously for the steady state.

C. Ultimate sensitivity

In the preceding section we evaluated the signal amplification. In this section we will evaluate the signal to noise ratio that determines the ultimate sensitivity of the LOFI detection technique.

1. Langevin noise terms

Without optical feedback ($\gamma_{\text{ext}}=0$), the set of Eqs. (1) allows us to study the laser fluctuations induced by the Langevin noise terms,

$$\frac{dN}{dt}=\gamma_1(N_0-N)-BN|E|^2+F_N(t),$$
$$\frac{dE}{dt}=\tfrac{1}{2}[BN-\gamma_c]E+F_E(t), \tag{15}$$

where $F_N(t)$ and $F_E(t)$ are the Langevin forces which describe the quantum fluctuations of the laser population and the radiation field. These forces are defined as having a zero mean value and white-noise-type correlation functions:

$$\langle F_m(t)\rangle=0,$$
$$\langle F_m(t)F_l(t')\rangle=D_{m,l}\delta(t-t'), \tag{16}$$

with $m,\ l\in[E,N]$ and with the following values for the diffusion coefficients [26]:

$$D_{E,E}=0s^{-1}, \tag{17a}$$

$$D_{E,E^*}=\frac{B\langle N\rangle}{2}+\frac{\gamma_c}{2}=\gamma_c, \tag{17b}$$

$$D_{N,N}=\gamma_1N_0+\gamma_1\langle N\rangle+B\langle N\rangle\langle|E|^2\rangle=2\gamma_c\eta\frac{\gamma_1}{B}. \tag{17c}$$

Finally, due to their common physical origin, the photon noise and the population inversion noise are perfectly anticorrelated and have a diffusion coefficient

$$D_{E,N}=-B\langle N\rangle\langle E\rangle=-\gamma_c\sqrt{\frac{\gamma_1}{B}(\eta-1)}. \tag{17d}$$

2. Laser quantum noise

In the same way as in Sec. II B 2, solutions for small fluctuations induced by the quantum noise can be obtained by linearization of Eqs. (15) around the steady states. We get the following equations:

$$\frac{d\Delta_N(t)}{dt}=-\eta\gamma_1\Delta_N(t)-\gamma_cE_S[\Delta_E(t)+\Delta_E^*(t)]+F_N(t),$$
$$\frac{d\Delta_E(t)}{dt}=\frac{1}{2}BE_S\Delta_N(t)+F_E(t). \tag{18}$$

Due to our choice of the steady-state solutions of the optical phase, the amplitude and optical phase fluctuations are, respectively, given by

$$\Delta_{E_C}(t)=\frac{\Delta_E(t)+\Delta_E^*(t)}{2},$$
$$\Delta_{\phi_c}(t)=\frac{1}{E_s}\frac{\Delta_E(t)-\Delta_E^*(t)}{2i}. \tag{19}$$

From the set of Eqs. (18), we obtain the following algebraic equations for the Fourier amplitudes of the laser fluctuations [with the definition $\Delta_X(\Omega)=(1/\sqrt{2\pi})\int_{-\infty}^{+\infty}\Delta_X(t)e^{i\Omega t}dt$]:

$$i\Omega\Delta_N(\Omega)=-\eta\gamma_1\Delta_N(\Omega)-\gamma_cE_S[\Delta_E(\Omega)+\Delta_E^*(-\Omega)]+F_N(\Omega),$$
$$i\Omega\Delta_E(\Omega)=\tfrac{1}{2}BE_s\Delta_N(\Omega)+F_E(\Omega). \tag{20}$$

The correlation functions of the Langevin forces are now given by [27]

$$\langle F_m(\Omega)F_l(-\Omega')\rangle=D_{m,l}\delta(\Omega-\Omega'). \tag{21}$$

The resolution of the linear set of Eqs. (20) is straightforward and leads to

$$\Delta_E(\Omega)=\frac{\left[\frac{1}{2}\omega_r^2-\Omega^2+i\Omega\eta\gamma_1\right]F_E(\Omega)-\frac{1}{2}\omega_r^2F_E^*(-\Omega)+i\Omega\frac{BE_s}{2}F_N(\Omega)}{i\Omega[\omega_r^2-\Omega^2+i\Omega\eta\gamma_1]}. \tag{22}$$

Due to the stationary optical phase choice (real field), the spectra of the fluctuation of the amplitude $\Delta_{E_c}(\Omega)$ and of the phase $\Delta_{\Phi_c}(\Omega)$ of the complex intracavity field $\Delta_E(t)$ are straightforwardly obtained from Eqs. (19)

$$\Delta_{E_c}(\Omega)=\frac{1}{2}[\Delta_E(\Omega)+\Delta_E^*(-\Omega)],$$
$$\Delta_{\Phi_c}(\Omega)=\frac{1}{2iE_s}[\Delta_E(\Omega)-\Delta_E^*(-\Omega)]. \tag{23}$$

The power density spectra of the amplitude $(\Delta_{E_c}^2)_\Omega$ and the optical phase $(\Delta_{\Phi_c}^2)_\Omega$ are obtained from their autocorrelation functions [27]

$$\langle\Delta_{E_c}(\Omega)\Delta_{E_c}(-\Omega')\rangle=2\pi(\Delta_{E_c}^2)_\Omega\delta(\Omega-\Omega'),$$
$$\langle\Delta_{\Phi_c}(\Omega)\Delta_{\Phi_c}(-\Omega')\rangle=2\pi(\Delta_{\Phi_C}^2)_\Omega\delta(\Omega-\Omega'), \tag{24}$$

and are given by using Eq. (22),

$$(\Delta^2_{E_c})_\Omega = \frac{1}{2\pi}\frac{\gamma_c}{2}\frac{\eta\gamma_1^2+\Omega^2}{(\omega_r^2-\Omega^2)^2+(\eta\gamma_1\Omega)^2},$$
$$(\Delta^2_{\Phi_c}) = \frac{1}{2\pi}\frac{1}{2|E_S|^2}\frac{\gamma_c}{\Omega^2}. \quad (25)$$

We can now use these expressions to calculate the signal to noise ratio of the LOFI signal.

3. Signal to noise ratio

For the amplitude, from Eqs. (11) and (25), we obtain the power density spectrum of the fluctuations of the output power due to the Langevin quantum noise,

$$A_{\text{noise}}(\Omega) \cong 4 n_{\text{out}} \gamma_c (\Delta^2_{E_c})_\Omega = 2\frac{n_{\text{out}}\gamma_c^2}{2\pi}\frac{\eta\gamma_1^2+\Omega^2}{(\omega_r^2-\Omega^2)^2+(\eta\gamma_1)^2\Omega^2}. \quad (26)$$

The power density spectrum of the LOFI signal is obtained from Eq. (12a)

$$A_{\text{signal}}(\Omega) = n_{\text{out}}^2\gamma_{\text{ext}}^2\frac{(\eta\gamma_1)^2+\Omega^2}{(\omega_r^2-\Omega^2)^2+(\eta\gamma_1)^2\Omega^2}\delta(\Omega-\Omega_0). \quad (27)$$

In the bandwidth Δ_Ω around the frequency Ω_0, the detected noise power and the detected signal power are then, respectively, given by

$$\langle [N_{\text{Ampl}}(\Omega_0)]^2\rangle = 2\int_{\Delta_\Omega} A_{\text{noise}}(\Omega)\,d\Omega,$$
$$\langle [S_{\text{Ampl}}(\Omega_0)]^2\rangle = 2\int_{\Delta_\Omega} A_{\text{signal}}(\Omega)\,d\Omega. \quad (28)$$

If the bandwidth of the detection is narrower than the resonance width ($\Delta_\Omega = 2\pi\Delta_F \ll \eta\gamma_1$), the power signal to noise ratio S/N of the amplitude of the modulation reduces to

$$S_{\text{Ampl}}/N_{\text{Ampl}} = \frac{p_{\text{out}}}{2\Delta_F}\frac{\gamma_{\text{ext}}^2}{\gamma_c^2}\frac{\eta^2\gamma_1^2+\Omega_0^2}{\eta\gamma_1^2+\Omega_0^2}. \quad (29)$$

Experimentally, in most cases, $\Omega_0 \gg \eta\gamma_1$ and the S/N is the independent of the frequency shift Ω_0. In that case, the minimum detectable effective reflection coefficient $R_{\text{eff}}^{\min}$ for a given signal to noise ratio is

$$R_{\text{eff}}^{\min} = \frac{2\Delta_F}{p_{\text{out}}}[S_{\text{Ampl}}/N_{\text{Ampl}}]. \quad (30)$$

Physically, this means that a $S/N=1$ is obtained when, during the integration time, only one photon is reinjected inside the laser cavity. The LOFI detection is therefore shot-noise limited. As an example, for an output beam of 1 mW at a wavelength of 1 μm, the minimum detectable value of the effective reflection coefficient $R_{\text{eff}}^{\min}$ could be as low as 2×10^{-13} for an integration time of 1 ms.

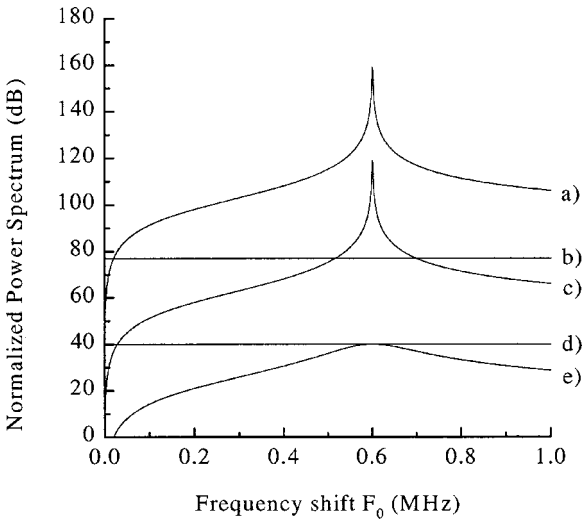

FIG. 4. Normalized theoretical power spectra of the output power of a reinjected laser versus the frequency shift ($F_0 = \Omega_0/2\pi$): (a) signal, (b) white detector noise, (c) laser quantum noise, (d) signal to noise ratio in the absence of detector noise (shot-noise limit), (e) signal to noise ratio including detector noise with $\eta=1.5$, $\gamma_1=5\times10^3\ \text{s}^{-1}$, $\gamma_c=5.7\times10^9\ \text{s}^{-1}$, $R_{\text{eff}}=10^{-14}$. Power spectra are normalized to the quantum shot noise ($p_{\text{out}}2\Delta F$) with the following parameters: $P=1$ mW, $\lambda=1$ μm, and $2\Delta F=1$ kHz.

Figure 4 shows the calculated power spectra [Eqs. (28)] of the output power of a frequency shifted reinjected laser. As we can see, the laser quantum noise, as well as the LOFI signal exhibit a strong resonance at the laser relaxation frequency. In the absence of detector noise the signal to noise ratio is frequency independent and also shot-noise limited. Now by including the detector noise presumed to be a white noise, the signal to noise ratio is only shot-noise limited within a frequency range close to the laser relaxation frequency (i.e., in a frequency domain where the laser quantum noise is several orders of magnitude higher than the detector noise).

For the optical phase, in the same way as for the amplitude, the power density spectra of the optical phase fluctuation is obtained from Eqs. (11) and (25):

$$P_{\text{noise}}(\Omega) \cong (\Delta^2_{\Phi_c})_\Omega = \frac{1}{2\pi}\frac{1}{n_{\text{out}}}\frac{\gamma_c^2}{\Omega^2}. \quad (31)$$

The power spectrum of the optical phase modulation is obtained from Eq. (12b),

$$P_{\text{signal}}(\Omega) = \frac{1}{4}\frac{\gamma_{\text{ext}}^2}{\Omega^2}\Delta(\Omega-\Omega_0). \quad (32)$$

In the bandwidth $\Delta\Omega$ around the frequency Ω_0, the detected optical phase signal and noise are then, respectively, given by

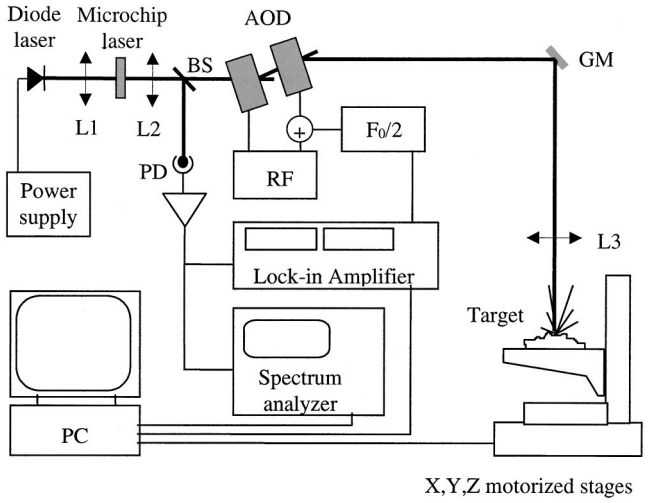

FIG. 5. Schematic diagram of the LOFI experiment: L1–L3, lenses; BS, beam splitter; PD photodiode; AOD, acousto-optic deflector; RF, radio-frequency generator; F_0, frequency shift; GM, galvanometric mirror.

$$\langle [S_{\text{phase}}(\Omega_0)]^2 \rangle = 2 \int_{\Delta\Omega} P_{\text{signal}}(\Omega) d\Omega,$$

$$\langle [N_{\text{phase}}(\Omega_0)]^2 \rangle = 2 \int_{\Delta\Omega} P_{\text{noise}}(\Omega) d\Omega. \tag{33}$$

The power signal to noise ratio is then given by the ratio of the two previous expressions,

$$S_{\text{phase}}/N_{\text{phase}} = \frac{p_{\text{out}}}{2\Delta F} \frac{\gamma_{\text{ext}}^2}{\gamma_c^2}. \tag{34}$$

As for the amplitude detection, the optical phase signal to noise ratio S/N is frequency independent. The optical phase detection is also shot-noise limited.

III. EXPERIMENTAL RESULTS

A. Experimental setup

The experimental setup is shown schematically in Fig. 5. The laser is a Nd^{3+}:YAG (yttrium aluminum garnet) microchip laser with a cavity length of 800 microns lasing at a wavelength of 1061.34 nm [28]. The pumping laser is a 810-nm diode laser. In typical operating conditions the threshold pump power is of the order of a few tens of mW. The maximum pump parameter available is about $\eta \approx 2$. For such conditions, the infrared output power is a few mW and the relaxation frequency $f_r = \omega_r/2\pi$ is in the range of 1 MHz.

The frequency shift is generated by means of two acousto-optic deflectors (AOD). The first is supplied by radio frequency (RF) at 81.5 MHz and the diffracted beam (order -1) is sent into the second AOD which is supplied by a RF at $(81.5 + F_0/2)$ MHz, where $F_0 = \Omega_0/2\pi$ is the frequency shift. Its diffracted beam (order $+1$) is therefore shifted by an optical frequency of $F_0/2$. The beam is then focused by a lens and sent to the target under investigation. All other beams are stopped by absorbing surfaces. The focused beam is diffracted and/or diffused by the target in the half space and only a small part of the retroreflected light is reinjected inside the laser cavity after a second pass through the frequency shifters. After this round trip the reinjected beam is then shifted by F_0. This frequency can by adjusted and is typically of the order of the laser relaxation frequency. Three-dimensional (3D) images can be obtained from the LOFI amplitude (reflectivity) [19] or from the LOFI phase (profilometry) [24]. Images are obtained either by moving the target in three dimensions using micrometric motorized stages or by moving the laser beam using a galvanometric scanner. In the latter case, the third dimension is then obtained by a Z micrometric motorized stage or by a variable focus lens [19].

A small fraction of the output beam of the microchip laser is sent to a Si-photodiode loaded by a 50Ω resistor. The delivered voltage is analyzed by a lock-in amplifier which gives directly the amplitude and the phase of the LOFI signal and/or by a spectrum analyzer. All these signals are a/d converted from analog to digital and recorded by a PC for further analysis and/or imaging.

B. Experimental observations

1. Laser quantum noise

Without optical feedback, the microchip laser exhibits in the time domain relatively strong fluctuations of the output intensity. As it was demonstrated in the theoretical section, these fluctuations, of the order of several percents, are mainly due to the resonant amplification of the Langevin quantum noise at the laser relaxation frequency.

Figure 6(a) shows a typical example of the time evolution of the laser output power where the relative fluctuation is of the order of $\Delta P_{\text{out}}/P_{\text{out}} = 40\%$. The inset shows clearly that laser quantum noise is mainly composed of quasiperiodic oscillations at the laser relaxation frequency. Figure 6(b) shows, for a microchip laser with an output power of 4 mW ($\eta = 1.7$, $n_{\text{out}} = 2 \times 10^{16}$ photon/s), a comparison between the experimental and the theoretical noise power spectrum of the laser. The experimental study of both the resonant frequency $\omega_r^2 = \gamma_1 \gamma_c (\eta - 1)$ and the full resonant width $\Delta\Omega = \gamma_1 \eta$ versus the pump parameter η allows us to determine the following laser damping rates: $\gamma_1 = 5 \times 10^3\ \text{s}^{-1}$ and $\gamma_c = 8 \times 10^9\ \text{s}^{-1}$ [29].

With these parameters, the theoretical noise power spectrum obtained from Eq. (26) is in good agreement with the experimental one. The discrepancies between the two curves at low and high frequency comes from the $1/F$ noise induced by the detection system and the harmonic noise induced by the nonlinear laser dynamics not included in the linear analytical development in Sec. II C 2.

For comparison, the power spectrum of the photodiode detector is also shown in Fig. 6. Far away from the $1/F$ noise, the laser quantum noise is several orders of magnitude higher than the detector noise. For a microchip laser, the LOFI detection system is then shot-noise limited in a broad frequency range around the laser relaxation frequency. This result is again a consequence of the very high value of the

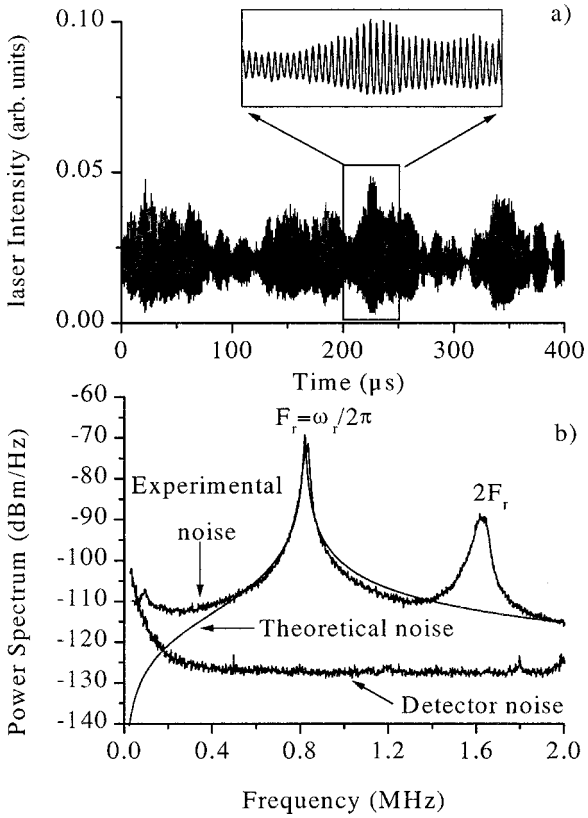

FIG. 6. (a) Typical time evolution of the Nd^{3+}: microchip laser without optical feedback. (b) Experimental and theoretical laser noise power spectrum with the following laser parameters: $\gamma_1=5\times10^3\ s^{-1}$, $\gamma_c=8\times10^9\ s^{-1}$, $\eta=1.7$, $P_{out}=4$ mW ($n_{out}=2\times10^{16}$ photon/s). The photodiode noise power spectrum is shown for comparison.

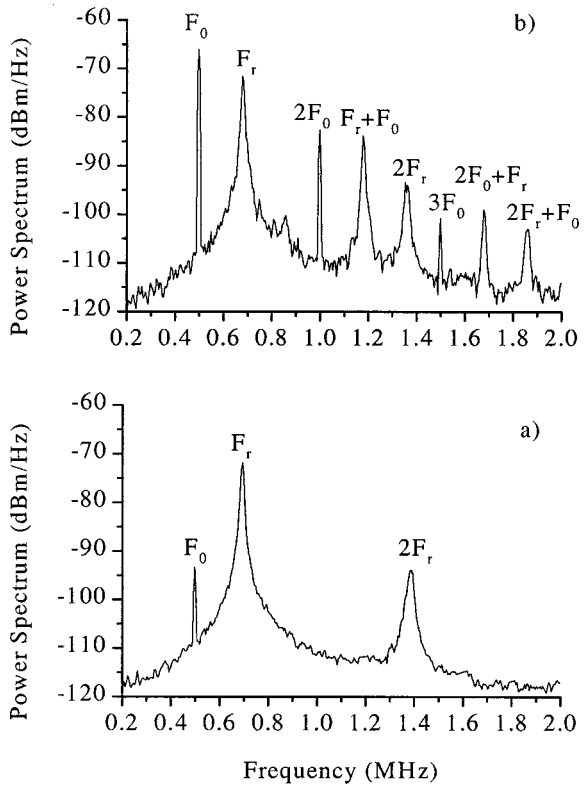

FIG. 7. Experimental power spectra of the laser output power with frequency-shifted optical feedback. (a) Weak optical feedback. (b) Strong optical feedback. For clarity of observation, the optical frequency shift F_0 is not resonant with the laser relaxation frequency F_r.

laser damping rate ratio ($\gamma_c/\gamma_1=1.6\times10^6$).

2. LOFI signal

With frequency-shifted optical feedback, the microchip laser exhibits in the time domain relatively strong oscillations of the output intensity. As it was demonstrated in the theoretical part, these fluctuations can be of the order of several percent for a feedback reflectivity as low as $R_{eff}=10^{-12}$.

Figure 7 shows typical experimental laser power spectra obtained with a spectrum analyzer. For weak optical feedback [Fig. 7(a)], the laser fluctuations are principally composed of the laser quantum noise at the relaxation frequency F_r and of the LOFI signal at the frequency F_0. For strong optical feedback, nonlinear dynamical effects appear in the laser output power. In these conditions, the power spectrum displays harmonic peaks ($2F_0,3F_0,\ldots$) and parametric peaks ($F_r+F_0,2F_r+F_0,2F_0+F_r,\ldots$).

C. Experimental analysis

The aim of this section is to confirm experimentally the behavior of the LOFI signal and the noise determined theoretically in Sec. I. Figure 8 compares the laser power spectra obtained for two different amounts of frequency-shifted optical feedback. The spectra are obtained by scanning the frequency shift and measuring with the lock-in amplifier.

For weak optical feedback, the laser quantum noise, as well as the LOFI signal, exhibit a strong resonance at the laser relaxation frequency. As predicted theoretically [Eq. (29) and Fig. 4], when the laser quantum noise is several orders of magnitude higher than the detector noise, the signal to noise ratio is frequency independent [Fig. 8(a)].

For strong optical feedback, when the optical frequency shift F_0 approaches the laser relaxation frequency F_r, the effects of nonlinear dynamics increase and there is a generation of harmonics, parametrics, and also probably chaotic laser oscillations. In this condition the LOFI signal at the frequency F_0 is completely saturated and the signal to noise ratio exhibits an antiresonance (i.e., a deep hole) at the laser relaxation frequency [Fig. 8(b)].

Figure 9 shows a study of the LOFI signal to noise ratio versus the effective reflectivity R_{eff}. Experimentally, the absolute value of R_{eff} is first calibrated by the study of the laser steady state. For strong optical feedback with zero-frequency shift, the change in the laser output power allows us to determine the external coupling coefficient γ_{ext} and then to calibrate R_{eff} [see Eqs. (2) and (6)].

The amount of optical feedback is then changed over several orders of magnitude by using calibrated optical attenuators. Figure 9 shows the normalized LOFI signal and the LOFI signal to noise ratio versus the effective reflectivity

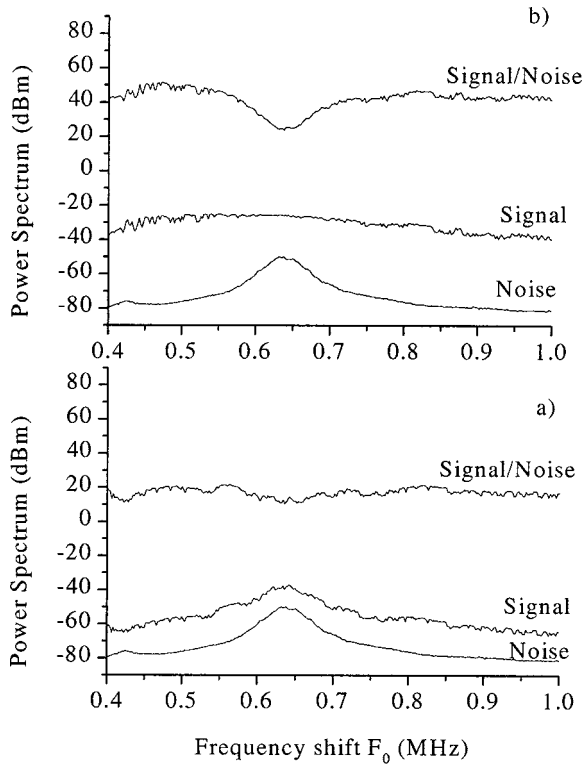

FIG. 8. Typical LOFI signal and laser noise versus the optical frequency shift. (a) For weak optical feedback the signal to noise ratio is approximately independent of the optical frequency shift. (b) For strong optical feedback the laser output oscillation at F_0 is completely saturated and the signal to noise ratio exhibits an antiresonance (i.e., a deep hole) at the laser relaxation frequency. Laser output power $P_{\text{out}}=4$ mW ($n_{\text{out}}=2\times10^{16}$ photon/s); lock-in integration time $T=1$ ms.

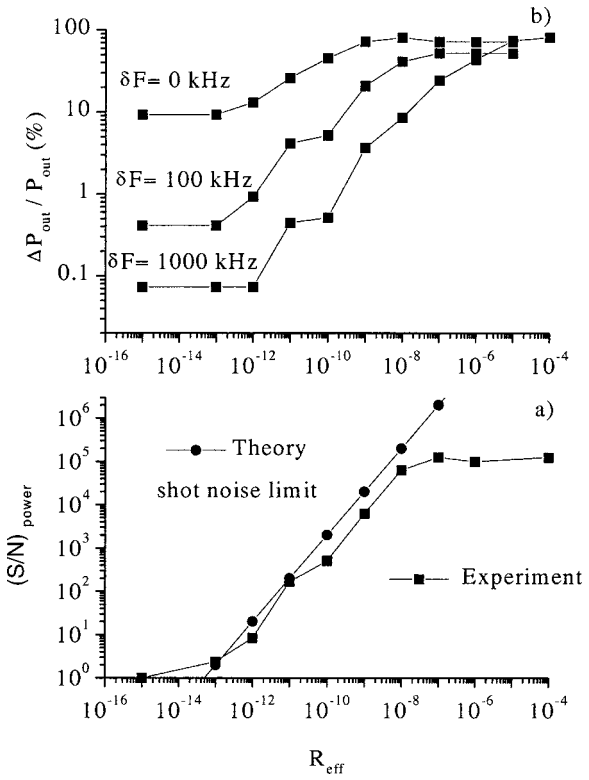

FIG. 9. LOFI signals measured with the lock-in amplifier versus the absolute effective reflectivity R_{eff} for different values of the detuning frequency $\delta F=F_0-F_r$. (a) Theoretical (shot-noise limit) and experimental power signal to noise ratio with $F_0=1200$ kHz and $F_r=900$ kHz. (b) Normalized LOFI signal $\Delta P_{\text{out}}/P_{\text{out}}$. Experimental conditions: laser output power, $P_{\text{out}}=4$ mW ($n_{\text{out}}=2\times10^{16}$ photons/s); lock-in integration time $T=1$ ms.

R_{eff} for different detuning frequencies ($\delta F=F_0-F_r$).

For a detuning frequency of $\delta F=300$ kHz [Fig. 9(a)], we observe that for over five orders of magnitude of the effective reflectivity ($10^{-13}\leqslant R_{\text{eff}}\leqslant10^{-8}$), experimental results are in good agreement with the theoretical result obtained from Eq. (30). On this graph, we can also observe that a signal to noise ratio equal to unity is obtained for a reflectivity of $R_{\text{eff}}\cong10^{-13}$. For these experimental conditions, this value corresponds to the shot-noise limit (one photon retroreflected is detected during the detection integration time).

In Fig. 9 we also observe that the saturation of the LOFI signal due to the nonlinear laser dynamics corresponds to a laser output modulation of approximately 80% and is independent of the frequency detuning δF. We also observe that the dynamic range of feedback detection increases with the frequency detuning. Indeed, for a microchip laser, due to the high value of the laser parameter ratio $\gamma_c/\gamma_1\cong1\times10^6$, the LOFI signal is rapidly saturated for a frequency shift close to the laser relaxation frequency.

IV. CONCLUSIONS

We have studied both theoretically and experimentally the dynamical response of a laser to frequency-shifted optical feedback and determined the ultimate sensitivity of the LOFI (laser optical feedback imaging) detection technique. In the LOFI technique, the beam of a laser is focused on or into a noncooperative target. Only photons backscattered from a volume located near the focus are reinjected by mode matching into the laser. The laser beam is frequency shifted before reinjection into the laser by a frequency F_0. The effect of the reinjected light is to modulate the net laser gain at the radio frequency F_0 and then to be amplified. The modulated intensity of the laser is detected by means of a lock-in amplifier or by a spectrum analyzer. The maximum amplification is obtained when the beating frequency F_0 is resonant with the relaxation oscillation frequency F_R of the laser. In such a condition, the relative modulation amplitude of the intensity is given by $\Delta P_{\text{out}}(F=F_R)/P_{\text{out}}=2(\gamma_c/\eta\gamma_1)\sqrt{R_{\text{eff}}}$, where η is the normalized pumping parameter, R_{eff} is the effective reflectivity of the target, and γ_c and γ_1 are, respectively, the cavity and the population inversion damping rates. Compared to a classical optical beating between two waves with the same relative amplitude, an amplification of γ_c/γ_1 occurs. This amplification is of the order of 10^6 for a microchip laser and 10^3 for a diode laser.

Experimentally, we have observed that for weak optical feedback, the laser fluctuations is principally composed of the laser relaxation frequency and of the LOFI signal at the frequency shift. For strong optical feedback, nonlinear ef-

fects appear in the laser dynamics. In these conditions, the laser power spectra exhibit harmonics and parametrics peaks. The LOFI signal at the optical frequency shift F_0 is then saturated.

Without optical feedback, the strong fluctuations of the microchip laser output power are well described by Langevin noise process. In a broad range around the laser relaxation frequency, the laser quantum noise is resonantly amplified and can be of several orders of magnitude higher than the detector noise. In these conditions, the LOFI technique is shot-noise limited. A reflectivity as low as 10^{-13} is then detectable with laser output power of a few mW in a detection bandwidth of 1 kHz.

ACKNOWLEDGMENTS

This study was supported by the Research-Industry Department of the University J. Fourier of Grenoble. The authors thank L. Fulbert and E. Molva of the Laboratoire d'Electronique de Technologie et d'Instrumentation/ Commisariat à l'Energie Atomique for providing the microchip lasers.

APPENDIX: DERIVATION OF EQ. (2)

Without optical feedback ($\gamma_{\text{ext}}=0$), and by neglecting internal losses (diffusion, parasitic absorption,...), the cavity damping rate is given by

$$\gamma_c=\frac{c}{2nl_c}\ln\left(\frac{1}{|r_1|^2|r_2|^2}\right), \tag{A1}$$

which in the case of $|r_1|^2=1$ and $|r_2|^2\approx 1$ reduces to

$$\gamma_c\approx\frac{c}{2nl_c}(1-|r_2|^2). \tag{A2}$$

The feedback parameter γ_{ext} appearing in Eq. (1) can be readly expressed in terms of the mirror reflection coefficient r_2 and the reflectivity r_3 of the target. If $E_i e^{i\omega t}$ is the intracavity incident field on the output mirror, then the total reflected field on this mirror, taking into account the reinjected field, is given by $E_r e^{i\omega t}=[r_2+(1-|r_2|^2)r_3 e^{-i\omega\tau}]E_i e^{i\omega t}$, where we have neglected multipass effects ($r_3\ll 1$). We can then define an effective amplitude reflectivity r_2^{eff} for the compound cavity as

$$r_2^{\text{eff}}=\frac{E_r}{E_i}=r_2\left[1+(1-|r_2|^2)\frac{r_3}{r_2}e^{-i\omega\tau}\right]. \tag{A3}$$

The effective cavity loss γ_c^{eff} of the compound cavity can be expressed as $\gamma_c^{\text{eff}}=(c/2nl_c)\ln(1/|r_1|^2|r_2^{\text{eff}}|^2)$, and by using Eqs. (A2) and (A3) we obtain

$$\gamma_c^{\text{eff}}=\gamma_c-\frac{c}{nl_c}(1-|r_2|^2)\frac{r_3}{r_2}e^{-i\omega\tau}\approx\gamma_c-2\gamma_c r_3 e^{-i\omega\tau}. \tag{A4}$$

In the above calculation, we have supposed that the system is autocollimated and therefore that the light reflected from the target is totally reinjected inside the laser cavity. For a target out of the focal point of the lens ($\delta\neq 0$), the system is no longer autocollimated (Fig. 1), and r_3 has to be multiplied by a normalized mode-matching coefficient g which takes into account the overlapping of the retroreflected electric field with the Gaussian cavity field. A similar situation happens if the target is not a mirror but a scattering medium; in this case g has to take into account the overlapping of the retrodiffused field with the Gaussian cavity beam. In both cases, this factor is of the following form [24]:

$$g(\delta)=\frac{\int\int\int_{\text{cavity}}|E_{\text{cavity}}||E_{\text{reinjected}}(\delta)dv|}{\int\int\int_{\text{cavity}}|E_{\text{cavity}}||E_{\text{cavity}}dv|}. \tag{A5}$$

In the hypothesis of a short focal length ($f\ll d_1$) and for a fundamental Gaussian beam, with a mirror as the target, a good approximation of Eq. (A5) is given by

$$g(\delta)\approx\left(\frac{1}{1+\frac{3\delta^2}{\Lambda^2}}\right)^{1/2}, \tag{A6}$$

where δ is the detuning between the focal point and the target (Fig. 1) and where $\Lambda=\sqrt{3}Z_R$, is the half width at half maximum (HWHM) and Z_R is the classical Rayleigh length defined by the numerical aperture of the focalizing lens.

The final expression of the effective cavity loss is then given by

$$\gamma_c^{\text{eff}}=\gamma_c-2g\gamma_c r_3 e^{-i\omega\tau}. \tag{A7}$$

From the above equation, by comparison with Eq. (1) one obtains the external coupling coefficient given by Eq. (2).

[1] R. Lang and K. Kobayashi, IEEE J. Quantum Electron. **QE-16**, 347 (1980).
[2] K. Otsuka and H. Kawaguchi, Phys. Rev. A **29**, 2953 (1984).
[3] P. Besnard, B. Meziane, and G. M. Stephan, IEEE J. Quantum Electron. **QE-29**, 1271 (1993).
[4] A. Bearden, M. P. O'Neil, L. C. Osborne, and T. L. Wong, Opt. Lett. **18**, 238 (1993).
[5] P. G. R. King and G. J. Steward, New Sci. **17**, 180 (1963).
[6] P. G. R. King and G. J. Steward, U.S. Patent No. 3,409,370 November 5, 1968.
[7] J. W. Campbell and V. Erbert, Appl. Opt. **6**, 1128 (1967).
[8] T. H. H. Peek, P. T. Bolwjin, and C. T. H. Alkemade, Am. J. Phys. **35**, 820 (1967).
[9] M. J. Rudd, J. Sci. Instrum. **1**, 723 (1968).

[10] N. Brown, Appl. Opt. **20**, 3711 (1981).
[11] D. Sarid, D. Iams, V. Weissenberger, and L. S. Bell, Opt. Lett. **13**, 1057 (1988).
[12] P. J. de Groot, J. Mod. Opt. **37**, 1199 (1990).
[13] D. Huang, J. Wang, C. P. Lin, J. S. Shuman, W. G. Stinson, W. Chang, M. R. Hee, T. Flotte, K. Gregory, C. A. Puliafito, and J. G. Fujimoto, Science **254**, 1178 (1991).
[14] D. A. Kleinman, Bell Syst. Tech. J. **43**, 1505 (1964).
[15] I. Fisher, O. Hess, W. Elsaher, and E. Gobel, Phys. Rev. Lett. **73**, 2188 (1994).
[16] Y. Liu and J. Ohtsubo, IEEE J. Quantum Electron. **QE-33**, 9371 (1997).
[17] E. Lacot, R. Day, and F. Stoeckel, Opt. Lett. **24**, 744 (1999).
[18] E. Lacot and F. Stoeckel, Patent No. WOFR9802092 (September 30, 1997).
[19] R. Day, E. Lacot, F. Stoeckel, and B. Berge, Appl. Opt. **40**, 1921 (2001).
[20] K. Otsuka, Jpn. J. Appl. Phys., Part 2 **31**, L1546 (1992).
[21] S. Okamoto, H. Takeda, and F. Kannari, Rev. Sci. Instrum. **66**, 3166 (1995).
[22] A. E. Siegman, *Lasers* (University Science Books, Mill Valley, CA, 1986).
[23] M. Sargent III, M. O. Scully, and W. E. Lamb, Jr., *Laser Physics* (Addison-Wesley, Reading, MA, 1974).
[24] R. Day, Ph.D. thesis, University J. Fourier, France, Dec. 2000.
[25] J. J. Zayhowsji and A. Mooradian, Opt. Lett. **14**, 24 (1989).
[26] M. I. Kolobov, L. Davidovich, E. Giacobino, and C. Fabre, Phys. Rev. A **47**, 1431 (1993).
[27] L. Mandel and E. Wolf, *Optical Coherence and Quantum Optics* (Cambridge University Press, Cambridge, 1995).
[28] M. Rabarot, J. Marty, L. Fulbert, Ph. Thony, and E. Molva, in *Conference on Lasers and Electro-Optics* (Optical Society of America, Washington, D.C., 1998), p. 483.
[29] S. Bielawsky, D. Derozier, and P. Glorieux, Phys. Rev. A **46**, 2811 (1992). For class-*B* lasers a better approximation of the damping rate of the relaxation oscillation (i.e., the resonance width) is given by

$$\Delta\Omega \cong \gamma_1 \eta + \frac{\gamma_c}{\eta - 1}\frac{B}{\gamma_1} = \gamma_1 \eta + \frac{\gamma_c^2}{n_{\text{out}}}.$$

Compared to the prediction of our simple rate equation model ($\Delta\Omega = \gamma_1 \eta$), the dramatic change of the resonance width near the threshold region ($\eta \approx 1$) is due to spontaneous emission. Fluorescence emission is known to give a significant contribution to the dynamics for guided lasers like semiconductor lasers or optical fiber lasers. In a microchip laser this effect is also important far away from the threshold ($\eta \approx 2$) due to the high value of the cavity damping rate γ_c compared to the population inversion damping rate γ_1.